Marine Geology 473 (2024) 107324

Contents lists available at ScienceDirect

Marine Geology

journal homepage: www.elsevier.com/locate/margo

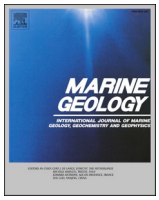

Research Article

The application of carbonate and sediment budgets to assess the stability of marginal reef systems

Shannon Dee [a,b,*], Adi Zweifler [c], Michael Cuttler [c,d,e], Jake Nilsen [a], Joshua Bonesso [c,f], Michael O'Leary [f], Nicola K. Browne [a,g]

[a] School of Molecular and Life Sciences, Curtin University, Kent St, Bentley, Western Australia 6102, Australia
[b] Centre for Marine Ecosystem Research, Edith Cowan University, 270 Joondalup Dr, Joondalup, Western Australia 6027, Australia
[c] Oceans Institute, The University of Western Australia, 35 Stirling Highway, Crawley, Western Australia 6009, Australia
[d] Oceans Graduate School, The University of Western Australia, 35 Stirling Highway, Crawley, Western Australia 6009, Australia
[e] Marine Energy Research Australia, 55 Proudlove Parade, Albany, Western Australia 6330, Australia
[f] School of Earth Sciences, University of Western Australia Oceans Institute, Western Australia 6009, Australia
[g] School of the Environment, University of Queensland, Brisbane, QLD 4072, Australia

ARTICLE INFO

Editor: Shu Gao

Keywords:
Carbonate budget
Sediment budget
Turbid reef
Sea level rise

ABSTRACT

Coral reefs and their associated landforms (carbonate islands and shorelines) are under increasing threat from the effects of anthropogenic climate change, including sea level rise (SLR). The ability of a reef to keep up with SLR depends on the rate of calcium carbonate accretion. Census-based carbonate budgets quantify rates of net calcium carbonate production on a reef and facilitate estimations of vertical reef accretion potential (RAP). To date, most carbonate budget studies have been undertaken in clear-water settings resulting in a limited understanding of how inshore reefs situated in more marginal environmental settings are functioning now and under future climate change. Here, we applied census-based carbonate framework across two inshore island reefs exposed to episodes of high turbidity within the Pilbara, Western Australia. Low net carbonate production (mean = 1.11 and 0.62 kg m^{-2} yr^{-1}) was predominantly driven by low coral cover (<10%) and low calcification rates. Importantly, bioerosion rates were also low (<0.1 kg m^{-2} yr^{-1}), maintaining positive carbonate budgetary states. Net sediment production rates were also low (mean = 0.06 kg m^{-2} yr^{-1}) and were found to be mostly derived from coral, or mollusc material produced by invertivores. Calculated RAP estimates are below current and predicted rates of SLR, suggesting that these turbid reefs will soon struggle to keep up with increasing water depth and shoreline inundation.

1. Introduction

Reef systems provide many ecological functions and are key habitats for a range of marine organisms, promoting biological diversity and supporting important economic and social functions (e.g., tourism, fisheries and culture; Kittinger et al., 2016). Reef accretion is largely driven by scleractinian corals (Perry and Alvarez-Filip, 2019), whose association with the symbiotic algae *Symbiodinium* promotes high rates of calcium carbonate production (Barott et al., 2014; Roth, 2014; Putnam et al., 2017). Reef carbonate production is also supported by other calcifying organisms such as crustose coralline algae (CCA), which help to build and stabilise the reef framework (Rasser and Riegl, 2002), as well as foraminifera, molluscs and *Halimeda,* which are direct sediment producers (Harney and Fletcher, 2003). These sediments either support reef construction (and accretion) by infilling the reef framework (Perry, 1999), or are transported towards shore contributing to landform building, or offshore into deeper waters (Sadd, 1984; Kench, 1998). Further, higher percentages of live coral cover is intrinsically linked to increased reef structural complexity, which in turn reduces wave energy and resultant coastal erosion of associated landforms (e.g., islands, beaches; Beck et al., 2018, Harris et al., 2018, Reguero et al., 2021). Reef growth and sediment production are, however, increasingly impacted by both warming temperatures and increasing ocean acidification (Crook et al., 2013; Cornwall et al., 2021). This has implications for the long-term stability of coral reefs and their associated landforms, as wave energy has a greater impact on shorelines if reef accretion rates are

* Corresponding author at: School of Molecular and Life Sciences, Curtin University, Kent St, Bentley, Western Australia 6102, Australia.
E-mail address: s.dee@ecu.edu.au (S. Dee).

https://doi.org/10.1016/j.margeo.2024.107324
Received 18 October 2023; Received in revised form 13 May 2024; Accepted 21 May 2024
Available online 23 May 2024

unable to keep up with rising sea-levels (Beetham et al., 2017).

The ecological processes that drive reef framework production and long-term stability can be assessed via census-based carbonate budgets, which estimate the net production of reef calcium carbonate. Reef carbonate inputs come from primary (scleractinian corals) and secondary (e.g. calcifying encrusters) sources, while the loss of carbonate from the framework occurs through physical, chemical, and biological erosion (see review by Browne et al., 2021). Reef-scale carbonate production and erosion can be estimated by combining abundances of calcifying and bioeroding organisms with taxa-specific calcification and erosion rates. This approach was first developed by Chave et al. (1972) and has since been adapted (see Perry et al., 2012, Perry et al., 2018a, 2018b) and used in over 50 studies globally, ~82% of which have occurred since the turn of the century (Table 1: Browne et al., 2021, and a further 17 additional published studies between 2021 and 2024). The rate of net carbonate production can be converted to an estimated rate of reef accretion potential (RAP, Perry et al., 2018a), using reef-specific sediment production and framework porosity values.

Although carbonate budgets are increasingly used to describe the health and function of reefs, distinct knowledge gaps remain. Firstly, there is a lack of diversity of studied reef type, with the majority (~90%) of census-based carbonate budget studies conducted on tropical clear-water reefs (e.g., Caribbean, Stearn and Scoffin, 1977; Sadd, 1984; Perry et al., 2013; de Bakker et al., 2019; Great Barrier Reef, Hamylton et al., 2013). In particular there have been relatively few carbonate budget studies of "marginal" reef systems such as turbid or polluted reefs (see blow). Secondly, it may be difficult or time consuming to collect site specific data which improve the accuracy of budget estimates (i.e., coral calcification rates; Browne et al., 2021). Thirdly, studies rarely incorporate carbonate sediment budgets (but see Perry et al., 2023: *SedBudget* method) despite the fact that carbonate budgets are associated with landform stability through the production of sediment on reefs (e.g., Perry et al., 2011; de Bakker et al., 2019; Kane and Fletcher, 2020; East et al., 2023). Lastly, very few studies have included environmental data (i.e. temperature, pH, salinity, light) reducing our ability to confidently relate how rates of net carbonate production and reef accretion may change under varying climate scenarios (Browne et al., 2021).

In the past two decades, less than ten census-based carbonate budget studies have been conducted on inshore reefs exposed to turbidity or urban pollution within the Indo-Pacific (e.g., Edinger et al., 2000; Browne et al., 2013; Herrán et al., 2017; Januchowski-Hartley et al., 2020;) and the Atlantic/ Caribbean (e.g., Mallela and Perry, 2007; Perry et al., 2012; Perry et al., 2013; Manzello et al., 2018). Inshore reefs are typically exposed to large fluctuations in turbidity, salinity, and temperature (Kleypas, 1996; Kleypas and McManu, 1999). These harsh conditions have led to the perception that these reefs are existing at their environmental limits and therefore support lower coral cover and diversity (Morgan et al., 2016, Schoepf et al., 2023). However, recent studies have recorded high levels of coral cover and diversity at sites exposed to high turbidity, as well as a capacity to withstand or quickly recover from disturbance events such as storms or heatwaves (Browne, 2012; Richards et al., 2015; Cacciapaglia and van Woesik, 2016; Guest et al., 2016; Lafratta et al., 2017; Morgan et al., 2017; Evans et al., 2020). With predicted impacts of anthropogenic climate change such as SLR, coupled with local stressors from coastal land-use change, turbidity on shallow in-shore reefs is expected to increase over the coming decades (Ogston and Field, 2010). As such, an improved understanding of how ecological drivers of carbonate production and erosion will respond to changing climatic conditions is becoming increasingly important for global reef conservation efforts.

Most carbonate budget studies to date have not included an assessment of reef carbonate sediment production. Knowledge on rates of carbonate sediment production (termed the carbonate sediment budget) and how they vary over space and time is critical to understanding the geo-ecological link between reefs and associated landforms (Kench and Cowell, 2006; Hamylton et al., 2016; Perry et al., 2023). A sediment budget includes rates of direct sediment production minus that lost through dissolution (Cyronak et al., 2013; Eyre et al., 2014; Andersson, 2015; Brown et al., 2021) and off reef transport (Kench, 1998; Browne et al., 2013; Morgan and Kench, 2014). Sediment budgets compliment the carbonate 'framework' budget as the type and size of sediment grains, and the rate of their production, is directly related to the

Table 1
Benthic habitat and environmental characteristics of each geomorphic zone together with the mean annual estimates of the environmental variables. Geomorphic zones of each reef are northern windward forereef (NWF; characterised by high cover of live coral and turfing algae), eastern leeward reef crest and forereef (ELC; characterised by high live coral cover), southern windward sandbar (SWS; dominated by macroalgae and rubble), southern leeward lagoon (SLL; high sand cover with occasional small coral bombie or sponges), and western windward forereef (WWF; consisting of high sediment cover with spurs and buttresses. Note that light and temperature were measured at the benthos at two sites per reef whereas chlorophyll-a, pH, salinity and turbidity were measured offshore of both Eva and Fly;).

Reef	Zone	Habitat size (m^2)	Average Rugosity	Depth (m)	Substrate cover (%)				Environment					
					Coral	MA	Old dead coral	Sand	Light (PAR)	Temperature (°C)	Chlorophyll (μg L^{-1})	pH	Turbidity (FNU)	Salinity
Eva	NWF	156,316	1.6	3.5	23	56	11	2	142.04 (±59.90)	27.15 (±0.80)	0.38 (±0.05)	8.18 (±0.01)	1.48 (±0.33)	38.16 (±0.42)
Eva	ELC	85,589	1.4	3.1	11	38	38	6	311.17 (±73.15)	27.15 (±0.80)				
Eva	SWS	125,198	1.3	3.6	2	65	4	11	142.04 (±59.90)	26.90 (±0.86)				
Eva	SLL	54,307	1.4	2.7	6	66	6	15	311.17 (±73.15)	26.90 (±0.86)				
Eva	WWF	182,116	1.3	3.4	5	55	6	13	142.04 (±59.90)	27.15 (±0.80)				
Fly	NWF	274,563	1.5	4.0	6	21	22	12	106.62 (±36.10)	27.20 (±0.89)	0.49 (±0.06)	8.19 (±0.03)	2.27 (±0.36)	38.34 (±0.46)
Fly	ELC	157,566	1.7	4.5	23	16	27	15	106.62 (±36.10)	27.20 (±0.89)				
Fly	SWS	429,132	1.1	3.1	0	73	0	19	127.08 (±65.53)	27.32 (±0.89)				
Fly	SLL	253,656	1.0	3.0	1	27	2	40	127.08 (±65.53)	27.32 (±0.89)				
Fly	WFF	334,414	2.1	2.7	1	48	17	5	106.62 (±36.10)	27.20 (±0.89)				

presence and abundance of sediment producing taxa, which are in turn dependent on the functions of the reef framework (Perry et al., 2011, 2023). The lack of inclusion of sediment budgets in carbonate budget studies is likely due to either: the difficulties in accurately assessing rates of sediment production and transport (see review by Browne et al., 2021); or the focus lies solely on framework carbonate production and reef health as opposed to the link between reefs and landforms. Nonetheless, there has been growing interest in applying sediment budgets to predict how unconsolidated carbonate landforms will respond to predicted SLR scenarios (de Bakker et al., 2019; Kane and Fletcher, 2020). These assessments require knowledge of carbonate sediment stocks and rates of sediment transport from reefs to islands to accurately make such predictions (Yamano et al., 2005; Kench and Cowell, 2006; Morgan and Kench, 2016; Cuttler et al., 2019).

This study aimed to produce comprehensive census-based carbonate budgets for two turbid reefs situated in northern Western Australia. Importantly, these reefs are associated with small reef islands (<60 ha; Bonesso et al., 2020) that endemic species (e.g., shore birds) and are of local cultural significance (e.g., Indigenous cultures and recreational activities; EPA, 2021). As such, our estimates of net carbonate production, RAP, and sediment production, provide some of the first insights into the long-term stability of these reefs and their associated islands. Further, we have provided a comprehensive environmental dataset that links ecological responses to environmental change.

2. Materials and methods

2.1. Regional setting

The southern Pilbara coast of Western Australia hosts >97 carbonate reef islands (Bonesso et al., 2020). The fringing reef systems that surround these inshore islands are exposed to frequent episodes of high turbidity (36.5 NTU), fluctuating ranges in temperature (18–32 °C) and salinity (35.4–39.6), and high energy storm events (e.g., tropical cyclones; McKenzie et al., 2009; Richards et al., 2016). Turbidity levels withing along the Pilbara coastline are result of fine sediments, which are deposited on large intertidal salt flats by north easterly winds, being flushed out into the coastal systems during spring tidal events, and resuspension from oceanic and wind driven swells (Cartwright et al., 2021).

This study was carried out across two inshore island reef systems, Eva (−21.918454°, 114.433502°) and Fly (−21.804829°, 114.554003°), situated at the mouth of the Exmouth Gulf (Fig. 1). Both reef systems have similar characteristics; specifically, the surrounding reef morphology can be described as a limestone platform which forms into a fringing reef around the northern edge of each island, a macroalgae and seagrass dominated sand bar forming off the south/southwest, and a sandy lagoon hosting small coral bombies around the south-east of each island.

2.2. Environmental data

Monthly water quality data (chlorophyll-a, conductivity, salinity, pH, turbidity) was collected offshore of each reef (Fig. 1) during neap tides between February 2019 and February 2020 (12 months). In situ sampling was undertaken using a vertical profiling method with a multiparameter EXO Sonde 2 (YSI Inc./Xylem Inc.), with detailed methods given in Dee et al. (2021). Temperature loggers (°C; Hobo Pendant UA-001-64) and photosynthetic active radiation (PAR) loggers (μmol photons m^{-2} s^{-1}; Odyssey submersible PAR logger) were deployed at each site from March 2019 to April 2020 (collected and replaced in September 2019) with logging intervals of 60 min for benthic temperature and 10 min for PAR loggers (Dee et al., 2021).

2.3. Reef geomorphology, habitats, and zones

To capture the variety of benthic habitats that surround each island, fifteen 20 m long photo line transects were laid parallel to the shore between 1 and 4 m depth. Details of image capture and benthic analysis are outlined in Dee et al. (2020). Following benthic identification, the marine habitats surrounding each island were sectioned into five 'zones' for spatial analysis and carbonate production calculations (Fig. 2). These zones included a northern windward forereef (NWF; characterised by high cover of live coral and turfing algae), eastern leeward reef crest and forereef (ELC; characterised by high live coral cover), southern windward sandbar (SWS; dominated by macroalgae and rubble), southern leeward lagoon (SLL; high sand cover with occasional small coral bombie or sponges), and western windward flat (WWF; consisting of high sediment cover with spurs and buttresses; Fig. 2; Table 1). In situ chain and tape rugosity measurements (*Rug*) were taken with a six-meter-long chain (links were 5 mm wide and 15 mm long) from the start of each transect, which were applied to calculate the three-

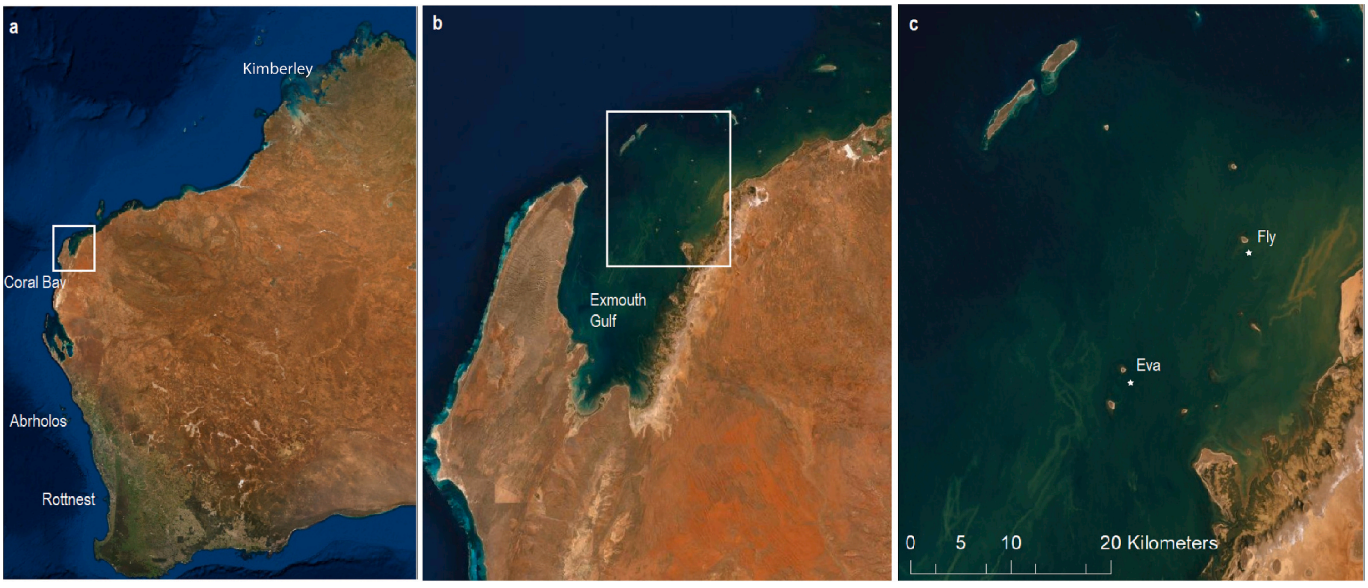

Fig. 1.. (a) Western Australia, showing location of Exmouth Gulf (b), situated at the southern end of the Pilbara region, and (c) the location of Eva and Fly islands. White stars indicate the location where water quality parameters (chlorophyll-a, pH, salinity and turbidity) were measured monthly.

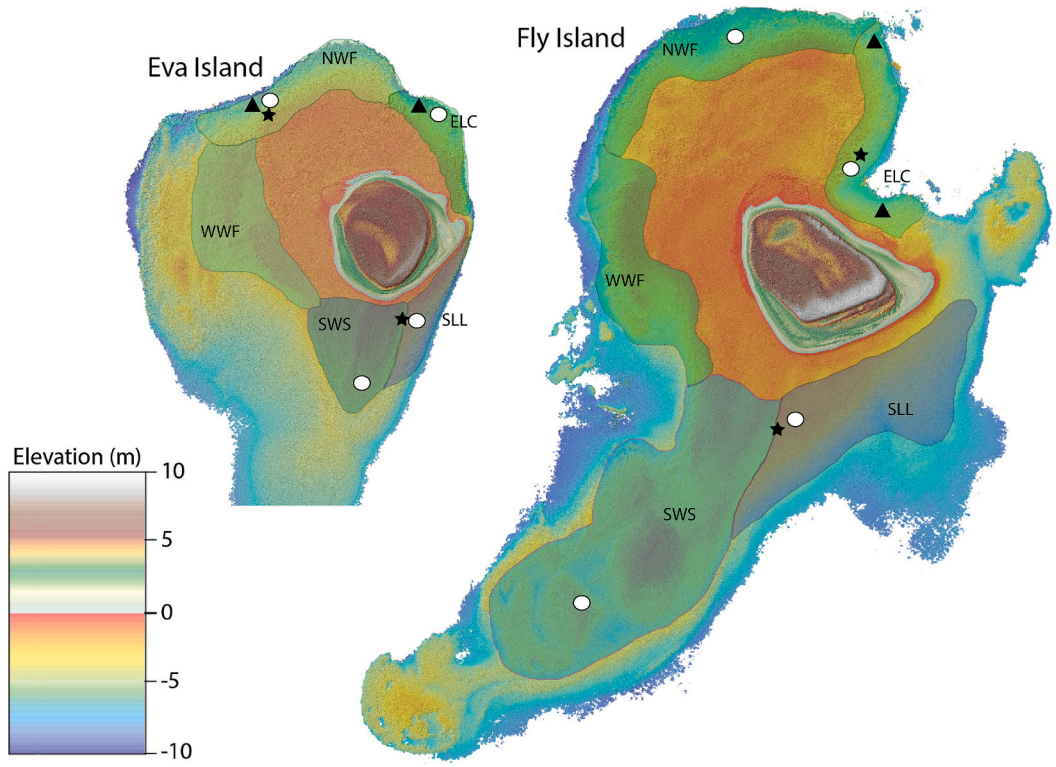

Fig. 2.. Bathymetric imagery of Fly and Eva reefs with transparent overlay displaying the range of each geomorphic reef zone. Reef zones include north windward forereef (NWF), east leeward crest (ELC), southern leeward lagoon (SLL), southern windward sandbar (SWS), and western windward forereef (WWF). White circles represent the location of encruster and bioerosion experiments, while black stars represent location of where temperature and light loggers were deployed at the benthos, and black triangles show the location of coral growth experiments.

dimensional habitat area (m^2) of each zone (A_Z);

$$A_Z = A \times Rug_Z \quad (1)$$

where A_Z is the zone habitat area (m^2), and Rug_z is the average rugosity measured from line transects within that zone, and (A) is the planimetric area of each zone (m^2). Planimetric area was measured from high resolution bathymetric LiDAR data (0.1 m; Dee et al., 2020).

2.4. Coral carbonate production

Calcification rates for *Acropora* spp. and *Pocillopora damicornis* were measured at four sites across Eva and Fly reefs using the buoyant weight method (Bak, 1973; Jokiel et al., 1978; Spencer Davies, 1989). These coral species were used as they are abundant across all zones of each reef, are easy to sample without damaging large sections of the colony, and are faster growing so are more reflective of environmental conditions at the time of budget assessment (Ross et al., 2017). Calcification rates for all other coral genera were sourced from literature (Table 2). Importantly, we included calcification rates from local studies (e.g., *Acropora, Pocillopora, Goniastrea, Favia, Porites, Turbinaria;* Foster et al., 2014; Dandan et al., 2015; Ross et al., 2015; Lough et al., 2016) and studies from inshore turbid reefs (e.g., Browne et al., 2013), where

Table 2
Coral calcification rates for each major coral genera recorded at Eva and Fly reefs. Here we compare the calcification rates of branching corals measured in situ with off-site rates from local studies (refs). Local calcification rates for some of the massive corals were available but were supplemented with studies outside of WA. Methodologies used to measure calcification rates were buoyant weight (BW), linear growth bands (LG) or coral core growth bands (CC). All rates of foliose and plating corals were only available from external studies. * Indicates calcification rate used in this study.

Morphology	Genus	Calcification Rate (g cm^{-2} yr^{-1})	Location	Method	Turbid reef setting	Source
Branching	*Acropora*	0.25*	Exmouth Gulf	BW	*	This study
		0.44	Pilbara and Kimberly	BW	*	Dandan et al. (2015)
		0.61	Rottnest Island	BW		Ross et al. (2015)
		0.42	Coral Bay	BW		Foster et al. (2014)
	Pocillopora	0.21*	Exmouth Gulf	BW	*	This study
		0.23	Rottnest Island	BW		Ross et al. (2015)
		0.34	Coral Bay	BW		Foster et al. (2014)
Foliose/plate	*Montipora*	1.52*	Inshore GBR	LG	*	Browne (2012)
	Turbinaria	1.37*	Inshore GBR	LG	*	Browne (2012)
		0.16	Bremer Bay	BW		Ross et al. (2019)
	Pavona	1.25*	Central Mexican Pacific	LG		Tortolero-Langarica et al. (2020)
Massive	*Porites*	1.62*	Pilbara Islands	CC	*	Lough et al. (2016)
	Goniastrea	0.45*	Coral Bay	BW		)Foster et al. (2014)
	Favia	0.37*	Pilbara and Kimberly	BW	*	Dandan et al. (2015)
	Lobophyllia	0.23*	Pilbara and Kimberly	BW	*	Dandan et al. (2015)
	Platygyra	1.10*	Persian Gulf	LG		Howells et al. (2018)

possible (Table 2).

A total of 30 coral fragments (15 *Acropora* and 15 *P.damicornis*) per reef were gathered in eastern and northern sites where coral cover is greatest, and transported to land where they were individually weighed in seawater and then attached to a PVC plate with marine epoxy. Once the epoxy was dry, corals were reweighed to determine the combined weight of the coral, plate and epoxy. Tiles were then attached to metal tripods ($n = 15$) and deployed at the fragment sampling sites (Fig. 2). After 13 months of deployment (September 2019–October 2020), approximately 40% of all coral nubbins had survived. The remaining live samples (total $n = 16$ *Acropora*, and 9 *P.damicornis*) were again buoyantly weighed and coral skeletal mass (g) were calculated using the following equation:

$$M_{air} = \frac{M_{sw} P_{CaCO3}}{P_{CaCO3} - P_{sw}} \quad (2)$$

Where M_{air} is the dry weight of the coral skeleton (g), M_{sw} is the mass of the sample in seawater (g; minus the weight of the tile and epoxy), and P_{CaCO3} and P_{sw} are the densities of coral and seawater, respectively (Jokiel et al., 1978). P_{sw} was measured each time samples were being weighed with a hydrometer, and P_{CaCO3} is the density of aragonite (2.93 g cm^3). Rates of coral carbonate production were calculated relative to coral surface area (Foster et al., 2014; Ross et al., 2019). The surface area of *Acropora* and *P.damicornis* samples were determined using the surface area to dry weight regressions from Foster et al. (2014), which was based on the same genera and species collected from a reef ~150 km to the south (Coral Bay; Fig. 1). Foster et al. (2014) found strong linear relationships between skeletal weight and colony surface area for *Acropora* ($R^2 = 0.98$) and *P.damicornis* ($R^2 = 0.97$).

Relative carbonate production of each coral genus (CCP; kg yr^{-1}) was calculated for each zone from the percent cover and mean calcification rate of each genus, multiplied by the habitat area (*Az*) of the zone as follows:

$$CCP = coral\% \times A_Z \times Calcification\ rate \quad (3)$$

Gross coral carbonate production ($\sum$CCP; Kg yr^{-1}) of each zone is then the sum of each genus CCP within a zone.

2.5. Encruster carbonate production

To obtain encruster carbonate production rates, encruster growth tiles were deployed at four locations around each of the two reefs (see Dee et al., 2021 for detailed methods). Tiles were deployed for 12 months, and once collected were dry weighed before and after being soaked in a dilute (10%) solution of hydrochloric acid (HCl) to dissolve all calcium carbonate. Tiles were then again rinsed, dried, and reweighed. Rates of encrusting carbonate production were calculated as follows:

$$\mathrm{ECR} = \left(\frac{(eg - ig)}{days} \div SA \right) \times 365 \quad (4)$$

Where ECR (kg m^{-2} yr^{-1}) is the rate of encrusters calcification, is calculated as the total mass (kg) of net carbonate accretion (end weight (*eg*) minus initial weight (*ig*)), divided by the deployment duration (*days*) and surface area of the tile (*SA,* m^2), and multiplied by 365 to provide annual rates (Mallela, 2013; Morgan and Kench, 2017). Zonal encruster carbonate production (ECP; kg yr^{-1}) was then calculated as the percent cover of CCA multiplied by the encrusting calcification rate (ECR; kg m^{-2} yr^{-1}), and the habitat area (A_z m^2) of each zone (Eq.5).

$$ECP = CCA\ cover\% \times encrusting\ calcification\ rate \times A_Z \quad (5)$$

CCA benthic cover (%) determined from the in situ transects was used to represent calcifying encruster abundance as CCA was the dominant encruster on the tiles (Dee et al., 2021). As tiles were not deployed in the western zones, we applied calcification rates of the northern zones, which had similar environmental (i.e., wave exposure, depth, light, temperature, substrate cover; Dee et al., 2020).

2.6. Gross carbonate production

Gross carbonate framework production (GF kg yr^{-1}) for each zone was calculated as the sum of the total mass produced by corals and encrusting organisms (Eq.6). The normalised gross framework production rate (GFN kg m^{-2} yr^{-1}) for each zone was calculated by dividing the total mass of carbonate produced by the zone area (Eq.7).

$$GF = \sum CCP + \sum ECP \quad (6)$$

$$GFN = GF \div A_Z \quad (7)$$

2.7. Framework bioerosion

Bioerosion monitoring units (BMU) were used to independently measure endolithic bioerosion across reef zones. Detailed methods can be found in Dee et al. (2023), but simply, 16 BMUs (2 × 5 × 1 cm) made from clean cores of *Porites lutea* were deployed across each reef for one year. Prior to deployment, BMUs were scanned using a Micro computed tomography (micro-CT; Skyscan1176, 90 kV, 273 μA), which was then repeated after collected BMUs were cleaned of organic matter to determine volume lost due to bioerosion. By comparing BMU carbonate volume before and after deployment, endolithic bioerosion rate (EBr; kg m^{-2} yr^{-1}) was calculated as:

$$EBr = (Vol_i \times P_i) \div (SA_i \times T) \quad (8)$$

where *i* refers to the individual BMU, Vol_i is the volume lost (m^3) during deployment, SA_i is the surface area of the BMU pre-deployment, P_i is the original density of the BMU pre-deployment, and T is the time in years that the unit was deployed for (DeCarlo et al., 2014; Silbiger et al., 2016).

External bioerosion (grazing) rates were quantified using urchin abundance estimates along 20 m transects (15 per reef) and diver-operated stereo-video (stereo-DOV) to collect data on fish abundance and biomass collected using a diver-operated stereo-video system (stereo-DOV) (Dee et al., 2023; also see Goetze et al., 2019). Stereo-DOV surveys were carried out along four 50 m transects with 10 m of separation at five sites across Eva Island ($n = 20$) (one survey among each WWF, ELC, SWS, and two among NWF zones). DOV surveys were not able to be undertaken at Fly reef, however grazing data from Eva was applied to the same zones of Fly as abundance of grazing parrotfish was observed to be similar. Bioerosion rates (BrN) for grazing parrot fish were determined using the Indo-Pacific data spreadsheet available from the *Reef Budget* website (Perry et al., 2018a; https://www.exeter.ac.uk/research/projects/geography/reefbudget/). Given very low urchin abundance across both reefs (<5 individuals per reef), urchins were excluded from the analysis. Gross bioerosion (GBrN) was the sum of endolithic bioerosion and grazing for each zone.

2.8. Reef accretion and growth

To calculate net carbonate framework production (*G,* kg m^{-2} yr^{-1}) the following equation was applied:

$$G = GFN - GBrN \quad (9)$$

Where GFN is the gross normalised framework carbonate production by corals and encrusting organisms, and GBrN is the gross normalised bioerosion rate by endolithic organisms and parrotfish across the zone. The reef accretion potential (RAP mm yr^{-1}; Eq. 12) for each zone is determined by dividing the net framework production (*G;* kg m^{-2} y^{-1}) by the weight of aragonite required for a reef to accrete 1 cm (29.3 kg) and correcting for reef porosity (Rpor) (Kinsey, 1985; Toth et al., 2022), which is taken as 20% as observed within reef cores extracted from

turbid zone reefs on the GBR (Palmer et al., 2010).

$$RAP = ((G \div 29.3) \div (100 - Rpor)) \times 1000 \quad (10)$$

2.9. Reef sediment budget estimates

Surficial sediment samples were taken from each transect location (15 samples), and were carefully collected with a scoop (250 cm^3) from the upper layer of a 10x10cm area of sand at the start of each transect and placed into a zip-lock bag. Sediments were soaked with bleach for 24 h to remove organic matter and then rinsed with distilled water and dried at 50 °C for 24 h before being weighed. Carbonate content was determined using approximately 5–7 g of the original sample to which 10% HCl solution was added to dissolve the calcium carbonate. After 24 h the non-carbonate residue was filtered through a pre-weighed 90 μm pore size filter paper using a suction filter and oven dried at 50 °C for 24 h. Once the filter paper was dry, the paper and the sample were reweighed. Carbonate content (%; Eq. 11) was calculated by subtracting the post-dissolved sample minus filter paper weight (S_p) from the pre-dissolved sample minus filter paper weight (S_i), divided by S_i and then multiplied by 100.

$$CaCO_3\% = \frac{(S_i - S_p)}{S_i} \times 100 \quad (11)$$

Sediment type was determined using a stereo microscope (Nikon SMZ745T). A subsample (~200 g) was dry sieved into five sieve fractions (<63 μm, 63–150 μm, 150–250 μm, 0.25–0.5 mm, 0.5–1 mm, 1–2 mm, >2 mm) and composition was assessed by identifying 100 sediment grains for each size class >150 μm as one of the following: hard coral, Mollusc (bivalve or gastropod), CCA, foraminifera, serpulid worms, crustacean, sponge spicules, echinoderm spine, unknown, or terrigenous. Sediment composition was expressed as the relative percentage abundance of the total sample and for each of the sieved sub-samples.

Direct carbonate sediment production (SPR, kg m^{-2} yr^{-1}) for each zone was assessed using the SedBudget methodology (Perry et al., 2023). Molluscs, CCA, foraminifera, and halimeda abundance data from photo transects and previous benthic quadrat surveys (see Bonesso et al., 2022), as well as sediment grain data, were applied to data sheets available from the SedBudget website (https://www.exeter.ac.uk/research/projects/geography/sedbudget/).

As detailed benthic quadrat surveys were not undertaken at Fly Reef, an accurate sediment budget could not be assessed for comparison.

Net sediment budget for Eva was calculated using gross sediment production minus the rate of sediment dissolution. Gross carbonate sediment production (GSP kg yr^{-1}) was determined by adding the annual amount of bioeroded sediment from macroborers and grazers (BrG) to the annual amount of carbonate sediments produced by the direct sediment producers (ASP). Sediment production rates by grazing parrotfish are considered to equate to bioerosion rates (Lange et al., 2020), assuming that all ingested material is excreted as sand (Bellwood, 1996). Sediment produced by macroborers is considered to be 80% of total macroboring as approximately 20% of eroded volume is estimated to be lost through chemical dissolution (Nava and Carballo, 2008). Rates from microborers were excluded as majority of microboring processes involve chemical dissolutions (i.e., no sediment is formed; Perry et al., 2017). GSP was then normalised by dividing by the habitat area (m^2, Eq. 12 and 13).

$$GSP = ASP + (BrG) \quad (12)$$

$$GSPN = GSP \div A_Z \quad (13)$$

To account for sediment dissolution for each zone, we used rates recorded in Brown et al. (2021) based on zone geomorphic setting. A sediment dissolution rate of 0.296 kg m^{-2} yr^{-1} was applied to forereef zones (NWF, ELC, WWF), while a rate of 1.07 kg m^{-2} yr^{-1} was applied for lagoonal settings (SLL, SWS; Brown et al., 2021). To calculate the final rate of sediment produced per zone (NSP; kg $m^{-2}y^{-1}$), we subtracted the appropriate sediment dissolution rate from the GSPN of each zone (Eq. 14)

$$NSP = GSPN - sediment\ dissolution\ rate \quad (14)$$

3. Results

3.1. Environment

Environmental variables had minimal variation between reefs, such as average benthic water temperature (Fly 24.9 ± 0.02 °C; Eva 24.8 ± 0.02 °C), salinity (Fly mean = 38.16 ± 0.42; Eva mean = 38.34 ± 0.46), and conductivity (Fly mean = 57,149 ± 982 μS cm^{-1}; Eva mean = 57,150 ± 965 μS cm^{-1};

3.2. Benthic community description

Benthic cover was comparable between reefs, with similar coral cover (8% at Fly, 10% at Eva) and fleshy algal cover dominating the benthos (macroalgae = 56% at Eva, and 35% at Fly; turfing algae = 16% at Eva, and 15% at Fly). Both reefs displayed distinct differences in benthic cover between south and north/east reef zones. Southern zones were characterised by higher macroalgae cover (52 and 67% for Fly and Eva, respectively) and exceptionally low coral cover (0–2%). Whereas northern and eastern zones displayed lower macroalgae cover (0–28%) and higher coral cover (29–37%), and high cover of turfing algae (16–35%), with the latter growing predominantly on dead coral substrate. Eva reef hosts a higher percentage of branching corals compared to Fly (Eva = 26%, Fly = 15%), whereas a higher percentage of massives were observed at Fly (Eva = 35%, Fly =45%), and an equal percentage of foliose corals between reefs (Eva = 39%, Fly = 40%; Fig. 3a). The highest coral cover recorded at Eva reef was 62% within the northern zone, while a maximum cover of 48% was recorded within the eastern zone of Fly reef. *Turbinaria* sp. displayed the greatest relative coral cover at each reef (~20% at Eva reef and 31% at Fly reef), followed by massive *Porites* spp. (16% at Eva and 17% at Fly; Fig. 3a). *Pocillopora* was the most common branching genera across both reefs (~15% at Eva and 12% at Fly; Fig. 3a).

3.3. Gross carbonate production

Coral calcification rates measured in this study were low (Acropora = 0.25 g cm^{-2} yr^{-1}, Pocillopora = 0.21 g cm^{-2} yr^{-1}), yet comparable to buoyant weight measures of these and other taxa along the Western Australian coast (Foster et al., 2014; Dandan et al., 2015; Ross et al., 2015, Table 2). As such, due to low coral cover and low calcification rates, Eva and Fly reefs had low average coral carbonate production rates (Eva = 0.97 ± 0.26 kg m^{-2} yr^{-1}, Fly = 0.54 ± 0.49 kg m^{-2} yr^{-1}). The zones of highest coral carbonate production were the northern zone (NWF) of Eva (2.54 ± 1.33 kg m^{-2} yr^{-1}) and the eastern zone (ELC) of Fly (2.03 ± 0.98 kg m^{-2} yr^{-1}), while the lowest coral carbonate production at both reefs was among the southern sand-bar zone (SWS; 0.08 ± 0.01 kg m^{-2} yr^{-1} and 0.00 kg m^{-2} yr^{-1} at Eva and Fly, respectively; Appendix A Table 1). Pavona produced the highest relative contribution to Eva reef's gross carbonate (~30%), while across both reefs Turbinaria (26–38%) and Porites (27–33%) also made up large contributions of calcium carbonate production (Fig. 3).

Average encruster carbonate production rates at Eva and Fly reef were 0.12 ± 0.05 kg m^{-2} yr^{-1} and 0.08 ± 0.03 kg m^{-2} yr^{-1}, respectively (Dee et al., 2021, Appendix A Table 1). The eastern zone (ELC) of Eva reef produced the highest average carbonate production rates (0.31 ± 0.01 kg m^{-2} yr^{-1}, while the southern zone (SWS) of each reef produced the lowest (0.03 ± 0.01 kg m^{-2} yr^{-1} at both reefs).

Total annual gross carbonate production was 239 × 10^3 kg yr^{-1} at Eva Reef of which 88% was produced by corals, and 125 × 10^3 kg yr-1 at Fly

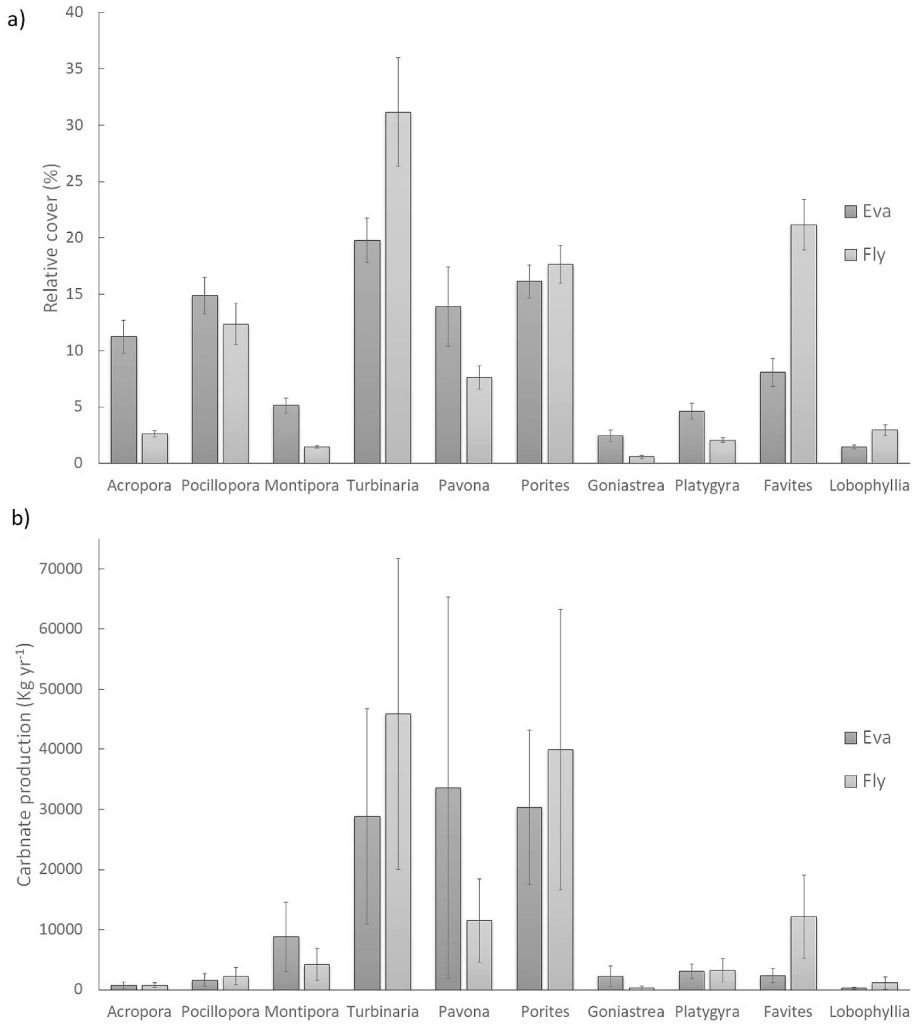

Fig. 3.. The relative cover (a) and contribution of each major coral genera to the overall coral carbonate production (b) at Eva and Fly reefs, error bars represent standard error.

reef, of which 82% was produced by corals. This equates to an average gross production rate of 1.11 + 0.26 and 0.62 + 0.49 kg m^{-2} y^{-1} at Eva and Fly reef, respectively.

3.4. Bioerosion

Mean normalised bioerosion rates were 0.07 ± 0.02 kg m^{-2} yr^{-1} at Eva, and 0.08 ± 0.02 kg m^{-2} yr^{-1} at Fly (Appendix A Table 2). Bioerosion by grazing parrotfish made up 51% of bioerosion at Eva reef, and 47% at Fly reef. The highest rates of total bioerosion were recorded in the WWF zone of each reef (~0.14 kg m^{-2} yr^{-1}), while the lowest rates of bioerosion were recorded at the NWF zone of Eva (0.04 kg m^{-2} yr^{-1}), and SLL of (0.02 kg m^{-2} yr^{-1}, Appendix A Table 2).

It is worth noting that endolithic bioerosion rates measured in this study are expected to be an underestimate due to the resolution of CT scans (microbioerosion) and the relatively short deployment period of BMUs across reef sides (i.e. 12 months for macrobioerosion).

3.5. Net carbonate framework production and accretion

Mean net carbonate framework production at Eva reef was 1.04 ± 0.45 kg m^{-2} yr^{-1}, while Fly displayed a mean net carbonate framework production rate of 0.55 ± 0.37 kg m^{-2} yr^{-1} (Fig. 4). Across Eva reef, net carbonate framework production ranged from 0.06 kg m^{-2} yr^{-1} in the SWS zone to 2.62 kg m^{-2} yr^{-1} in the NWF zone. Net carbonate framework production at Fly ranged from 0.00 kg m^{-2} yr^{-1} in the SWS zone to 1.96 kg m^{-2} yr^{-1} in the ELC (Fig. 4).

The average RAP across the entire Eva Reef was 0.44 ± 0.19 mm yr^{-1}, while Fly Reef had a lower average RAP of 0.19 ± 0.13 mm yr^{-1} (Appendix A Table 3). The NWF zone of Eva Reef showed the greatest RAP at 1.12 mm yr^{-1}, followed by the ELC and SLL zones both at 0.47 mm yr^{-1}. At Fly, the ELC zone showed the greatest RAP at 0.67 mm yr^{-1}. The SWS zone of each reef showed the lowest RAP (Eva = 0.02 mm yr^{-1}; Fly = 0.00 mm yr^{-1}; Appendix A Table 3).

3.6. Direct sediment production

Sediments collected from Eva were classified as coarse sand and consisted of ~95% carbonate. The two dominant components at Eva were coral fragments (~37%) and mollusc materials (34%, Appendix A Table 4). Sediments consisted of approximately 6% CCA and ~ 7% foraminifera, with the remaining contents made up of spicules, crustacean, serpulid, bryozoan, echinoderm and terrigenous materials.

Average direct sediment production was 0.90 ± 0.19 kg m^{-2} yr^{-1}. Mollusc made up the majority of benthic taxa that would contribute to sediment productions, with rates from halimedia and live foraminifera being almost negligible.

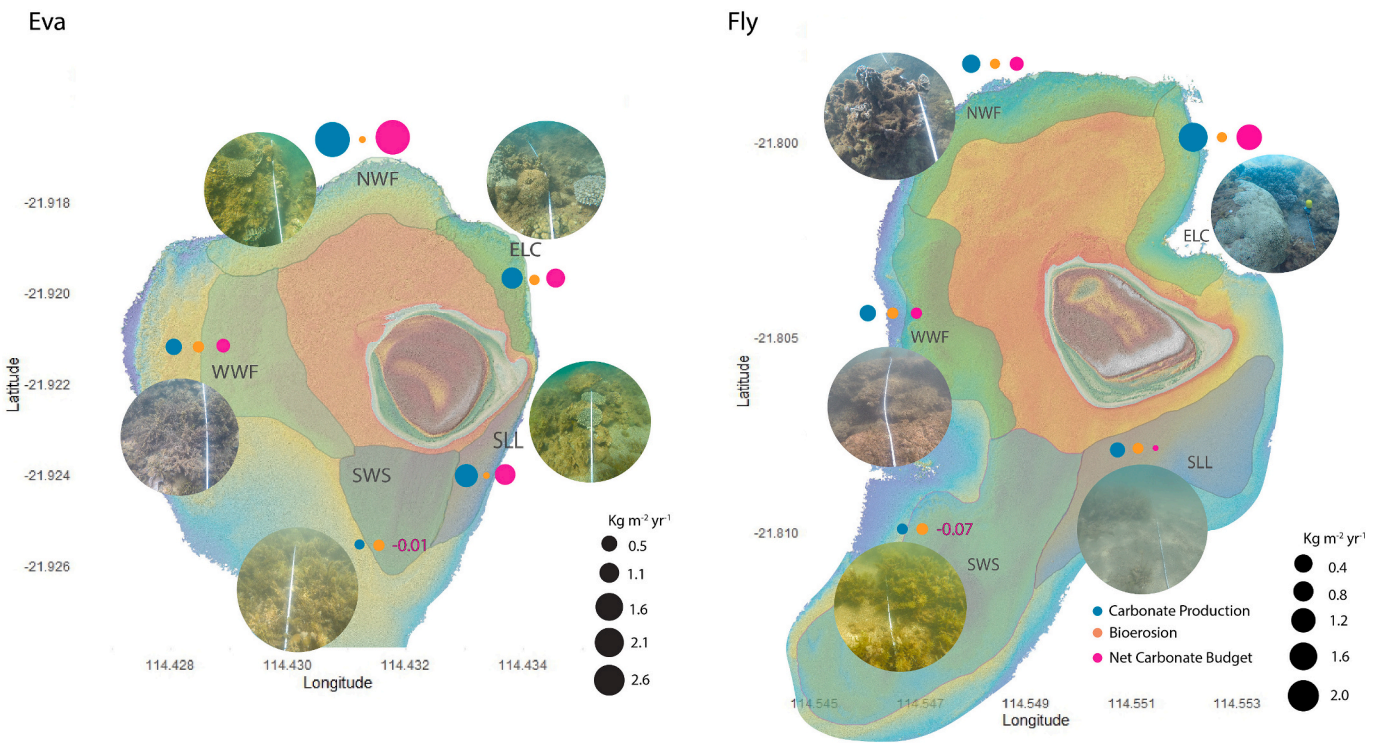

Fig. 4.. Benthic habitat and estimated carbonate production, bioerosion, and net carbonate budget (kg m^{-2} yr^{-1}) for each geomorphic reef zone of Eva and Fly reefs.

3.7. Net carbonate sediment production

Across Eva reef, the average amount of bioeroded sediment produced from macroborers and grazers was 7.40 ± 3.67 × 10^3 kg yr^{-1} (Table 3). When combined with estimates of direct sediment produced on the reefs, the average normalised gross sediment production rate of Eva reef was 0.06 ± 0.02 kg m^{-2} yr^{-1}. Taking sediment dissolution into account, rate of net sediment production at Eva reef is −0.55 kg m^{-2} yr^{-1}.

4. Discussion

4.1. Pilbara islands reef carbonate budgets

Eva and Fly reefs currently have a low but positive reef budgetary state with net carbonate framework production at 1.04 ± 0.45 and 0.55 ± 0.37 kg m^{-2} yr^{-1}, respectively. In contrast, neighbouring Ningaloo Reef, which lies in the clear waters off the western side of the Exmouth peninsula, was estimated to have a greater net carbonate production rate between 1.4 and 3.9 kg m^{-2} yr^{-1} (see Perry et al., 2018b). Rates of net carbonate production measured in this study are, however, comparable to some carbonate budget states recorded among turbid or polluted reefs of the Indo-Pacific and Caribbean. A recent study on Singapore's inshore turbid reefs recorded a low mean net carbonate budget of 0.68 kg m^{-2} yr^{-1} (Januchowski-Hartley et al., 2020), while Mallela and Perry (2007) recorded net carbonate budget rate of 1.89 kg m^{-2} yr^{-1} at an inshore Jamaican reef site exposed to riverine induced turbidity, and de Backker et al. (2019) recorded average rates of 0.58 and 0.85 kg m^{-2} yr^{-1} at urban reefs of Bonaire heavily influenced by anthropogenic pressures. These comparisons between polluted and turbid settings support previous assumptions that the southern Pilbara reefs are existing within marginal environmental settings despite a lack of local anthropogenic stressors.

4.2. Carbonate production rates

In this study, we recorded average calcification rates of 0.25 g cm^{-2} yr^{-1} for Acropora spp. and 0.21 g cm^{-2} yr^{-1} for *Pocillopora damicornis*, which were comparable to rates measured in local studies using the same buoyant weight methodology. For example, Dandan et al. (2015) measured an Acropora calcification rate of 0.44 g cm^{-2} yr^{-1} within the Pilbara and similarly turbid Kimberly region to the north. While Foster et al. (2014) recorded an Acropora calcification rate of 0.42 g cm-2 yr-1 and *P. damicornis* growth rates of 0.34 g cm-2 yr-1 in near by clear water Coral Bay (Fig. 1). Further south, Ross et al. (2015) recorded growth rates for *P. damicornis* of 0.23 g cm-2 yr-1 at Rottnest Island, a high latitude reef. It is well acknowledged that using local growth rates will increase the accuracy of census-based reef carbonate production

Table 3
Sediment budget for Eva reef including calculated gross sediment production (kg cm^{-2} yr^{-1}) from direct sediment production and sediment derived from bioerosion, estimated sediment dissolution rates (kg cm^{-2} yr^{-1}), and net carbonate sediment production rates for each geomorphic zone.

	Direct sediment production kg m^2 yr^{-1}	Bioeroded sediment production kg m^2 yr^{-1}	Normalised Gross Carbonate sediment production kg m^{-2} yr^{-1}	Sediment dissolution kg m^{-2} yr^{-1}	Net Carbonate sediment production kg m^{-2} yr^{-1}
Eva					
NWF	0.007	0.03	0.03	0.30	−0.26
ELC	0.006	0.07	0.08	0.30	−0.22
SWS	–	0.03	0.03	1.07	−1.04
SLL	–	0.03	0.03	1.07	−1.04
WWF	0.006	0.12	0.13	0.30	−0.17
Mean ± ***se***	**0.006 ± <0.001**	**0.06 ±**	**0.06 ± 0.02**	**0.61 ± 0.19**	**−0.55 ± 0.19**

estimates (Perry et al., 2018a; Browne et al., 2021). This may not always be possible given that assessment of coral growth rates require longer time frames (several months) than many in situ benthic surveys require. In these situations, it is encouraged that growth rates from similar reef settings (e.g. clearwater, turbid, high latitude etc.) be substituted into the carbonate calculations.

Accurate carbonate production estimates also rely on assessing the true surface area of the benthos and coral cover. There are two approaches that can be used to incorporate this element. The first approach, which was used here, was to measure reef rugosity using the chain and tape method. The second approach is to measure the total coral colony contour of each coral colony that intercept the transect line. This approach is more accurate as it calculates calcification on a colony-level and has been updated for the ReefBudget method (Perry et al., 2012; Perry et al., 2018a). No comparisons have been made between these two approaches to assess if they differ significantly and if these differences are consistent between reef habitats characterised by different coral community compositions. It is likely that there will be some differences but until this research is undertaken it cannot be determined which approach is more appropriate. However, care should be taken when comparing data between the different approaches.

4.3. Bioerosion rates

Much like coral carbonate production rates, bioerosion rates across Eva and Fly reefs were also low compared to previous studies. Average total bioerosion rates were 0.07 kg m-2 yr-1 at Eva and 0.08 kg m-2 yr-1 at Fly. Bioerosion rates vary spatially from inshore to offshore (Sammarco and Risk, 1990; Cooper et al., 2008), with inshore sites typically experiencing higher macroboring and lower external grazing than offshore reefs (Tribollet et al., 2002; Hutchings et al., 2005). High sedimentation and turbidity on inshore reefs are known to negatively affect the abundance of herbivorous reef fish (Cheal et al., 2013), reducing what can be a dominant driver of bioerosion rates. Within this study we observed very low numbers of parrot fish (13 total) between 11 and 30 cm in length, which indicated low grazing rates. However, parrotfish species abundance is known to vary with tides and time of day, and so it is possible DOV transects conducted throughout the middle of the day may not have captured the full extent of the local population. Although personal observations over a number of years and rare sightings of grazing scars on corals over multiple field expeditions support the assumption that parrotfish populations are low within Exmouth Gulf.

Sedimentation may also inhibit the settlement and development of microboring taxa such as endolithic algae (Hutchings et al., 2005). In contrast, higher rates of macro-boring on inshore reefs has been linked to higher levels of nutrients in coastal waters (Edinger et al., 2000; Le Grand and Fabricius, 2011). As such, previous carbonate budget studies conducted on reefs close to urban centres (e.g., Singapore, Januchowski-Hartley et al., 2020; Jepara, Edinger et al., 2000; Townsville Browne et al., 2013) have found macro-borers to be the dominant bioeroding group. In this study, rates of macro bioerosion were comparatively low (0.02 kg m^{-2} yr^{-1} at Eva and 0.03 kg m^{-2} yr^{-1} at Fly), which could potentially be appointed to the lack of local anthropogenic pressure (e.g., urban runoff, pollutants, nutrients) and to the short timeframe of block deployment (compared to other studies which usually deploy for 3+ years). Under this “natural” setting, low bioerosion pressure has facilitated a positive budgetary state despite low net carbonate production.

4.4. Spatial variations and environmental pressure

Carbonate production and removal varied spatially within and between both reefs. In particular, Eva reef showed the greatest rates of carbonate production, potentially driven by higher average light levels measured at this reef. In contrast, Fly reef was exposed to higher levels of turbidity and chlorophyll-a, which may have hindered carbonate production rates as well as increased endolithic bioerosion (Le Grand and Fabricius, 2011). Rates of bioerosion were, however, greater in the WWF and SWW zones of each reef. These small-scale (1 to 10 km) spatial differences highlight the variation in reef habitat types around islands, and how net carbonate production differs between them. It is therefore essential that island reef carbonate budget studies include all surrounding habitats (see also; Hamylton, 2014; Hamylton and Mallela, 2019; Ryan et al., 2019). In doing so, it is likely that predictions of how reefs and associated islands may respond to changing environmental and hydrodynamic conditions into the future will improve (Cuttler et al., 2020; Masselink et al., 2020; Masselink et al., 2021).

Small-scale spatial differences in production rates also highlight the need for caution when up-scaling rates of net carbonate production from a limited number of transects to whole reef systems. A potential approach that could improve the upscaling of carbonate budgets to reef systems is to develop empirical relationships that describe how key ecological processes that drive budgets (e.g., calcification rates, bioerosion) are responding to individual and interacting environmental drivers. These quantified relationships could then be combined with remotely sensed habitat maps to estimate net carbonate production at the reef scale and better predict future rates of change (Hamylton et al., 2013).

4.5. Sediment budget

The carbonate sediment budget of Eva reef is low at 0.06 ± 0.02 kg m-2 yr-1. This rate is comparably low to clear water as well as turbid studies within the Indo-Pacific. For example, net sediment production rate of 2.82 kg m-2 yr-1 has been estimated for Heron Island reef on the southern GBR (Brown et al., 2021). Further, sediment production quantified in this study is also a magnitude lower than that of turbid inshore reefs of the GBR (~0.2 kg m-2 yr-1 Browne et al., 2013).

It has been well established that parrotfish are leading producers of carbonate sediments within tropical clear water reefs (Bellwood, 1996), but this is not always the case for other reef types. For example, reef sediments have been found to be dominated by fragments of Halimeda spp. (e.g., Timor Sea, North-western Australia; Hayward et al., 1997), foraminifera (e.g. Green Island and Raine Island, North-eastern Australia; Yamano et al., 2000; Dawson et al., 2014) and molluscs (e.g. Lagoonal waters of New Caledonia; Chevillon, 1996), highlighting the role of other organisms in carbonate sediment production and supply. Here we found that reef sediments were largely made up on mollusc material (>30%), which is also reflected within sediments collected from the associated reef islands (Bonesso et al., 2022). Nilsen et al. (2022) identified invertivores as the dominant feeding guild (based on biomass) at Eva reef, and their gut contents were >95% carbonate material (e.g. molluscs, echinoderms).

The low rate of sediment production at Eva reef is expected to be an underestimate as sediment production as key invertivore species were not taken into account when applying the ReefBudget or SedBudget methodologies. While these methods include invertivore fish types such as trigger fish and puffer fish, they do not currently include tusk fish species such as *Choerodon cyanodus* and *Choerodon schoenleinii*, as well as emperor species *Lethrinus laticaudis*, which all feed on molluscs, yet no feeding rates could be found in the literature. This highlights there is more research required to fully understand the role of invertivore fish in sediment production particularly within more turbid waters where these fish guilds may be more abundant.

An additional limitation to quantifying a sediment budget within this study is the lack of onsite dissolution data, as well as the lack of sediment transport estimates. As stated above, these can be difficult to accurately estimate, and the required field logistics were not achievable during this study due to travel restrictions.

4.6. Reef accretion and future island stability

Reef accretion potential (RAP) rates varied between 0.00 and 1.11 mm yr-1 with an average rate of 0.45 ± 0.19 mm yr-1 for Eva and 0.19 ± 0.12 mm yr-1 for Fly reef. These estimates fall below even the most conservative global mean SLR prediction of 4.4 mm yr-1 under the International Panel on Climate Change (IPCC) Representative Concentration Pathway (RCP) scenario 2.6, and is well below current globally averaged SLR of approximately 3 mm yr-1 (Church and Gregory, 2019). Within in Pilbara coast line in Northwest Western Australia, RCP scenario 2.6 predicts a sea level increase of 0.39 m by 2090, with scenario 4.5 predicting an increase of 0.46 m by 2030. Under these expected water level increases and tidal ranges in this region (2–3 m), increased water depth above reef substrate will result in increased wave energy reaching the island shore, and hence increasing impacts of wave-driven erosion (Storlazzi et al., 2015; Kane and Fletcher, 2020). Ultimately, there remains a level of uncertainty regarding how reefs will respond to SLR as well as how islands and sediment regimes will be altered under predicted SLR and hydrodynamic scenarios in conjunction with, as well as independent of RAP (East et al., 2018, 2020; Masselink et al., 2020; Tuck et al., 2021).

Recent research into the morpho-dynamics of Eva and Fly islands showed that these islands have remained stable over the past two decades, despite displaying dynamic morphological responses to seasonal shifts in wave climate and water levels (Cuttler et al., 2020). Bonesso et al. (2020) showed that the reef platform area of Eva and Fly reef was directly linked to the net volume of their associated islands, with a larger platform area providing a greater sediment factory and direct sediment feed (also see East et al., 2018). In this scenario, RAP may have smaller impact on rates of direct sediment feed as majority of sediment production is expected to be derived from predation on molluscs in the surrounding habitat. If this is the case, Eva and Fly may sustain island stability into the future through positive sediment production, although this scenario is far more likely under combined environmental variables supportive of positive carbonate budget states.

Funding

This research study was supported by an Australian Research Council (ARC) Discovery Project DP160102561; and a DECRA Fellowship DE180100391 awarded to Nicola Browne of Curtin University, Perth, as part of the island resilience project (2018–2020).

CRediT authorship contribution statement

Shannon Dee: Writing – review & editing, Writing – original draft, Methodology, Investigation, Formal analysis, Data curation, Conceptualization. **Adi Zweifler:** Writing – review & editing, Methodology, Investigation. **Jake Nilsen:** Methodology, Investigation. **Joshua Bonesso:** Data curation, Investigation. **Michael O'Leary:** Writing – review & editing, Methodology, Investigation. **Nicola K. Browne:** Writing – review & editing, Supervision, Methodology, Investigation, Funding acquisition, Conceptualization.

Declaration of competing interest

The authors declare the following financial interests/personal relationships which may be considered as potential competing interests:

Nicola Browne reports financial support was provided by Australian Research Council.

Data availability

The data presented in this study are available at https://data.mendeley.com/datasets/tjrrsm8nmr/3

Acknowledgements

The authors would like to acknowledge Brooke Gibbons, Savita Goldsworthy, Tahlia Basset and Trent Bradshaw for their assistance in the field, as well as the Minderoo Foundation for their support.

Appendix A. Supplementary data

Supplementary data to this article can be found online at https://doi.org/10.1016/j.margeo.2024.107324.

References

Andersson, A.J., 2015. A fundamental paradigm for coral reef carbonate sediment dissolution. Front. Mar. Sci. 2, 1–8. https://doi.org/10.3389/fmars.2015.00052.

Bak, R.P.M., 1973. Coral weight increment in situ. A new method to determine coral growth. Mar. Biol. 20, 45–49. https://doi.org/10.1007/BF00387673.

de Bakker, D.M., van Duyl, F.C., Perry, C.T., Meesters, E.H., 2019. Extreme spatial heterogeneity in carbonate accretion potential on a Caribbean fringing reef linked to local human disturbance gradients. Glob. Chang. Biol. 25, 4092–4104. https://doi.org/10.1111/gcb.14800.

Barott, K.L., Venn, A.A., Perez, S.O., Tambutté, S., Tresguerres, M., 2014. Coral host cells acidify symbiotic algal microenvironment to promote photosynthesis. Proc. Natl. Acad. Sci. 112 (2), 607–612. https://doi.org/10.1073/pnas.1413483112.

Beck, H.E., Zimmermann, N.E., McVicar, T.R., Vergopolan, N., Berg, A., Wood, E.F., 2018. Present and future Köppen-Geiger climate classification maps at 1-km resolution. Scient. Data 5, 180214. https://doi.org/10.1038/sdata.2018.214.

Beetham, E., Kench, P.S., Popinet, S., 2017. Future Reef Growth can Mitigate Physical Impacts of Sea-Level rise on Atoll Islands. Earth's Future 5, 1002–1014. https://doi.org/10.1002/2017EF000589.

Bellwood, D.R., 1996. Production and reworking of sediment by parrotfishes (family Scaridae) on the Great Barrier Reef, Australia. Mar. Biol. 125, 795–800.

Bonesso, J.L., Cuttler, M.V.W., Browne, N., Hacker, J., O'Leary, M., 2020. Assessing reef island sensitivity based on LiDAR-derived morphometric indicators. Remote Sens. 12, 3033. https://doi.org/10.3390/rs12183033.

Bonesso, J.L., Browne, N.K., Murley, M., Dee, S., Cuttler, M.V.W., Paumard, V., Benson, D., O'Leary, M., 2022. Reef to island sediment connections within an inshore turbid reef island system of the eastern Indian Ocean. Sediment. Geol. https://doi.org/10.1016/j.sedgeo.2022.106177.

Brown, K.T., Bender-Champ, D., Achlatis, M., van der Zande, R.M., Kubicek, A., Martin, S.B., Castro-Sanguino, C., Dove, S.G., Hoegh-Guldberg, O., 2021. Habitat-specific biogenic production and erosion influences net framework and sediment coral reef carbonate budgets. Limnol. Oceanogr. 66, 349–365. https://doi.org/10.1002/lno.11609.

Browne, N.K., 2012. Spatial and temporal variations in coral growth on an inshore turbid reef subjected to multiple disturbances. Mar. Environ. Res. 77, 71–83. https://doi.org/10.1016/j.marenvres.2012.02.005.

Browne, N.K., Smithers, S.G., Perry, C.T., 2013. Carbonate and terrigenous sediment budgets for two inshore turbid reefs on the central Great Barrier Reef. Mar. Geol. 346, 101–123. https://doi.org/10.1016/j.margeo.2013.08.011.

Browne, N.K., Cuttler, M.V.W., Moon, K., Morgan, K.M., Ross, C.L., Castro-Sanguino, C., Kennedy, E.V., Harris, D.L., Barnes, P., Bauman, A.G., Beetham, E.P., Bonesso, J., Bozec, Y., Cornwall, C.E., Dee, S., Decarlo, T.M., D'olivo, J.P., Doropoulos, C., Evans, R.D., Eyre, Bradley D., Gatenby, P., Gonzalez, M., Hamylton, S., Hansen, J.E., Lowe, R.J., Mallela, J., O'Leary, M.J., Roff, George, Saunders, B.J., Zweifler, A., 2021. Predicting responses of geological carbonate reef systems to climate change: A conceptual model and review. Oceanography and Marine Biology, pp. 229–370.

Cacciapaglia, C., van Woesik, R., 2016. Climate-change refugia: Shading reef corals by turbidity. Glob. Chang. Biol. 22, 1145–1154. https://doi.org/10.1111/gcb.13166.

Cartwright, P.J., Fearns, P.R.C.S., Branson, P., Cuttler, M.V.W., O'Leary, M., Browne, N. K., Lowe, R.J., 2021. Identifying metocean drivers of turbidity using 18 years of MODIS satellite data: implications for marine ecosystems under climate change. Remote Sens. 13 (18), 3616. https://doi.org/10.3390/rs13183616.

Chave, K.E., Smith, S.V., Roy, K.J., 1972. Carbonate production by coral reefs. Mar. Geol. 12, 123–140. https://doi.org/10.1016/0025-3227(72)90024-2.

Cheal, A.J., Emslie, M., MacNeil, M.A., Miller, I., Sweatman, H., 2013. Spatial variation in the functional characteristics of herbivorous fish communities and the resilience of coral reefs. Ecol. Appl. 23, 174–188. https://doi.org/10.1890/11-2253.1.

Chevillon, C., 1996. Skeletal composition of modern lagoon sediments in New Caledonia: coral, a minor constituent. Coral Reefs 15, 199–207. https://doi.org/10.1007/BF01145892.

Church, J.A., Gregory, J.M., 2019. Sea level change. Encycl. Ocean Sci. 493–499 https://doi.org/10.1016/B978-0-12-409548-9.10820-6.

Cooper, T.F., Ridd, P.V., Ulstrup, K.E., Humphrey, C., Slivkoff, M., Fabricius, K.E., 2008. Temporal dynamics in coral bioindicators for water quality on coastal coral reefs of the Great Barrier Reef. Mar. Freshw. Res. 59, 703–716. https://doi.org/10.1071/MF08016.

Cornwall, C.E., Comeau, S., Kornder, N.A., Perry, C.T., van Hooidonk, R., DeCarlo, T.M., Pratchett, M.S., Anderson, K.D., Browne, N., Carpenter, R., Diaz-Pulido, G., D'Olivo, J.P., Doo, S.S., Figueiredo, J., Fortunato, S.A.V., Kennedy, E., Lantz, C.A., McCulloch, M.T., González-Rivero, M., Schoepf, V., Smithers, S.G., Lowe, R.J., 2021. Global declines in coral reef calcium carbonate production under ocean acidification

and warming. Proc. Natl. Acad. Sci. USA. https://doi.org/10.1073/pnas.2015265118.
Crook, E.D., Cohen, A.L., Rebolledo-Vieyra, M., Hernandez, L., Paytan, A., 2013. Reduced calcification and lack of acclimatization by coral colonies growing in areas of persistent natural acidification. Proc. Natl. Acad. Sci. USA 110, 11044–11049. https://doi.org/10.1073/pnas.1301589110.
Cuttler, M.V.W., Hansen, J.E., Lowe, R.J., Trotter, J.A., McCulloch, M.T., 2019. Source and supply of sediment to a shoreline salient in a fringing reef environment. Earth Surf. Process. Landf. 44, 552–564. https://doi.org/10.1002/esp.4516.
Cuttler, M.V.W., Vos, K., Branson, P., Hansen, J.E., O'Leary, M., Browne, N.K., Lowe, R. J., 2020. Interannual response of reef islands to climate-driven variations in water level and wave climate. Remote Sens. 12, 1–18. https://doi.org/10.3390/rs12244089.
Cyronak, T., Santos, I.R., Eyre, B.D., 2013. Permeable coral reef sediment dissolution driven by elevated pCO 2 and pore water advection. Geophys. Res. Lett. 40, 4876–4881. https://doi.org/10.1002/grl.50948.
Dandan, S.S., Falter, J.L., Lowe, R.J., McCulloch, M.T., 2015. Resilience of coral calcification to extreme temperature variations in the Kimberley region, Northwest Australia. Coral Reefs 34, 1151–1163. https://doi.org/10.1007/s00338-015-1335-6.
Dawson, J.L., Smithers, S.G., Hua, Q., 2014. The importance of large benthic foraminifera to reef island sediment budget and dynamics at Raine Island, northern Great Barrier Reef. Geomorphology 222, 68–81. https://doi.org/10.1016/j.geomorph.2014.03.023.
DeCarlo, T.M., Cohen, A.L., Barkley, H.C., Cobban, Q., Young, C., Shamberger, K.E., Brainard, R.E., Golbuu, Y., 2014. Coral macrobioerosion is accelerated by ocean acidification and nutrients. Geology 43, 7–10. https://doi.org/10.1130/G36147.1.
Dee, S., Cuttler, M., O'Leary, M., Hacker, J., Browne, N., 2020. The complexity of calculating an accurate carbonate budget. Coral Reefs 39, 1525–1534. https://doi.org/10.1007/s00338-020-01982-y.
Dee, S., Cuttler, M., Cartwright, P., McIlwain, J., Browne, N., 2021. Encrusters maintain stable carbonate production despite temperature anomalies among two inshore island reefs of the Pilbara, Western Australia. Mar. Environ. Res. https://doi.org/10.1016/j.marenvres.2021.105386.
Dee, S., DeCarlo, T., Lozić, I., Nilsen, J., Browne, N.K., 2023. Low bioerosion rates on inshore turbid reefs of Western Australia. Diversity 15, 62. https://doi.org/10.3390/d15010062.
East, H.K., Perry, C.T., Kench, P.S., Liang, Y., Gulliver, P., 2018. Coral reef island initiation and development under higher than present sea levels. Geophys. Res. Lett. https://doi.org/10.1029/2018GL079589, 45,11,265–11,274.
East, H.K., Perry, C.T., Beetham, E.P., Kench, P.S., Liang, Y., 2020. Modelling reef hydrodynamics and sediment mobility under sea level rise in atoll reef island systems. Glob. Planet. Chang. 192, 103196 https://doi.org/10.1016/j.gloplacha.2020.103196.
East, H.K., Johnson, J.A., Perry, C.T., et al., 2023. Seagrass meadows are important sources of reef island-building sediment. Commun. Earth Environ. 4, 33. https://doi.org/10.1038/s43247-023-00675-y.
Edinger, E.N., Limmon, G.V., Jompa, J., Widjatmoko, W., 2000. Normal Coral Growth Rates on Dying Reefs : Are Coral Growth Rates Good Indicators of Reef Health ?, vol. 40, pp. 404–425.
EPA, 2021. Potential Cumulative Impacts of Proposed Activities and Developments on the Environmental, Social and Cultural Values of Exmouth Gulf in Accordance with Section 16 (e) of the Environmental Protection Act 1986.
Evans, R.D., Wilson, S.K., Fisher, R., Ryan, N.M., Babcock, R., Blakeway, D., Bond, T., Dorji, P., Dufois, F., Fearns, P., Lowe, R.J., Stoddart, J., Thomson, D.P., 2020. Early recovery dynamics of turbid coral reefs after recurring bleaching events. J. Environ. Manag. 268, 110666 https://doi.org/10.1016/j.jenvman.2020.110666.
Eyre, B.D., Andersson, A.J., Cyronak, T., 2014. Benthic coral reef calcium carbonate dissolution in an acidifying ocean. Nat. Clim. Chang. 4, 969–976. https://doi.org/10.1038/nclimate2380.
Foster, T., Short, J.A., Falter, J.L., Ross, C., Mcculloch, M.T., 2014. Reduced calcification in Western Australian corals during anomalously high summer water temperatures. J. Exp. Mar. Biol. Ecol. 461, 133–143. https://doi.org/10.1016/j.jembe.2014.07.014.
Goetze, J.S., Bond, T., McLean, D.L., Saunders, B.J., Langlois, T.J., Lindfield, S., Fullwood, L.A.F., Driessen, D., Shedrawi, G., Harvey, E.S., 2019. A field and video analysis guide for diver operated stereo-video. Methods Ecol. Evol./Br. Ecol. Soc. 10 (7), 1083–1090. https://doi.org/10.1111/2041-210X.13189.
Guest, J.R., Low, J., Tun, K., Wilson, B., Ng, C., Raingeard, D., Ulstrup, K.E., Tanzil, J.T.I., Todd, P.A., Toh, T.C., McDougald, D., Chou, L.M., Steinberg, P.D., 2016. Coral community response to bleaching on a highly disturbed reef. Sci. Rep. 6, 1–11. https://doi.org/10.1038/srep20717.
Hamylton, S., 2014. Will Coral Islands maintain their growth over the Next Century? A Deterministic model of sediment availability at Lady Elliot Island, Great Barrier Reef. PLoS One 9 (4), e94067. https://doi.org/10.1371/journal.pone.0094067.
Hamylton, S., Silverman, J., Shaw, E., 2013. The use of remote sensing to scale up measures of carbonate production on reef systems: a comparison of hydrochemical and census-based estimation methods, 34, 6451–6465.
Hamylton, S.M., Mallela, J., 2019. Reef development on a remote coral atoll before and after coral bleaching: a geospatial assessment. Mar. Geol. 418. https://doi.org/10.1016/j.margeo.2019.106041.
Hamylton, S.M., Carvalho, R.C., Duce, S., Roelfsema, C.M., Vila-Concejo, A., 2016. Linking pattern to process in reef sediment dynamics at Lady Musgrave Island, southern Great Barrier Reef. Sedimentology 63, 1634–1650. https://doi.org/10.1111/sed.12278.
Harney, J.N., Fletcher, C.H., 2003. A budget of carbonate framework and sediment production, Kailua Bay, Oahu, Hawaii. J. Sediment. Res. 73, 856–868. https://doi.org/10.1306/051503730856.
Harris, D.L., Pomeroy, A., Power, H., Casella, E., Rovere, A., Webster, J.M., Parravicini, V., Canavesio, R., Collin, A., 2018. Coral reef structural complexity provides important coastal protection from waves under rising sea levels. Sci. Adv. 4, 7. https://doi.org/10.1126/sciadv.aao4350.
Hayward, B.W., Hollis, C.J., Grenfell, H.R., 1997. Recent Elphidiidae (Foraminiferida) of the South-West Pacific and Fossil Elphidiidae of New Zealand (No Title).
Herrán, N., Narayan, G.R., Reymond, C.E., Westphal, H., 2017. Calcium carbonate production, coral cover and diversity along a distance gradient from Stone Town: a case study from Zanzibar, Tanzania. Front. Mar. Sci. 4 https://doi.org/10.3389/fmars.2017.00412.
Howells, E., Dunshea, G., McParland, D., Vaughan, G.O., Heron, S.F., Pratchett, M.S., Burt, J.A., Bauman, A.G., 2018. Species-specific Coral calcification responses to the extreme environment of the Southern Persian Gulf. Front. Mar. Sci. 56. https://nsuworks.nova.edu/occ_facarticles/1302.
Hutchings, P., Peyrot-Clausade, M., Osnorno, A., 2005. Influence of land runoff on rates and agents of bioerosion of coral substrates. Mar. Pollut. Bull. 51, 438–447. https://doi.org/10.1016/j.marpolbul.2004.10.044.
Januchowski-Hartley, F.A., Bauman, A.G., Morgan, K.M., Seah, J.C.L., Huang, D., Todd, P.A., 2020. Accreting coral reefs in a highly urbanized environment. Coral Reefs 39, 717–731. https://doi.org/10.1007/s00338-020-01953-3.
Jokiel, P.L., Maragos, J., Franzisket, L., 1978. Coral growth: buoyant weight technique. Coral Reefs Res. Methods 529–541.
Kane, H.H., Fletcher, C.H., 2020. Rethinking reef island stability in relation to anthropogenic sea level rise. Earth's Futur. https://doi.org/10.1029/2020EF001525.
Kench, P.S., 1998. Physical controls on development of lagoon sand deposits and lagoon infilling in an Indian Ocean atoll. J. Coast. Res. 14, 1014–1024.
Kench, P.S., Cowell, P.J., 2006. Variations in Sediment Production and Implications for Atoll Island Stability under Rising Sea Level.
Kinsey, D.W., 1985. Metabolism, calcification and carbon production I: system level studies. Proceedings of the Fifth International Coral Reef Congress. Tahiti 4, 505–526.
Kittinger, J.N., Bambico, T.M., Minton, D., Miller, A., Mejia, M., Kalei, N., Wong, B., Glazier, E.W., 2016. Restoring ecosystems, restoring community: socioeconomic and cultural dimensions of a community-based coral reef restoration project. Reg. Environ. Chang. 16, 301–313. https://doi.org/10.1007/s10113-013-0572-x.
Kleypas, J.A., 1996. Coral reef development under naturally turbid conditions: fringing reefs near Broad Sound, Australia. Coral Reefs 15, 153–167. https://doi.org/10.1007/BF01145886.
Kleypas, J.A., McManu, J.W., 1999. Environmental limits to coral reef development: where do we draw the line? Am. Zool. 39, 146–159. https://doi.org/10.1093/icb/39.1.146.
Lafratta, A., Fromont, J., Speare, P., Schönberg, C.H.L., 2017. Coral bleaching in turbid waters of North-Western Australia. Mar. Freshw. Res. 68, 65–75. https://doi.org/10.1071/MF15314.
Lange, I.D., Perry, C.T., Morgan, K.M., Roche, R., Benkwitt, C.E., Graham, N.A., 2020. Site-Level Variation in Parrotfish Grazing and Bioerosion as a Function of Species-Specific Feeding Metrics. Diversity 12, 379. https://doi.org/10.3390/d12100379.
Le Grand, H.M., Fabricius, K.E., 2011. Relationship of internal macrobioeroder densities in living massive porites to turbidity and chlorophyll on the Australian Great Barrier Reef. Coral Reefs 30, 97–107. https://doi.org/10.1007/s00338-010-0670-x.
Lough, J.M., Cantin, N.E., Benthuysen, J.A., Cooper, T.F., 2016. Environmental drivers of growth in massive porites corals over 16 degrees of latitude along Australia's northwest shelf. Limnol. Oceanogr. 61, 684–700. https://doi.org/10.1002/lno.10244.
Mallela, J., 2013. Calcification by reef-building sclerobionts. PLoS One 8, 1–13. https://doi.org/10.1371/journal.pone.0060010.
Mallela, J., Perry, C.T., 2007. Calcium carbonate budgets for two coral reefs affected by different terrestrial runoff regimes, Rio Bueno, Jamaica. Coral Reefs 26, 129–145. https://doi.org/10.1007/s00338-006-0169-7.
Manzello, D.P., Enochs, I.C., Kolodziej, G., Carlton, R., Valentino, L., 2018. Resilience in carbonate production despite three coral bleaching events in 5 years on an inshore patch reef in the Florida Keys. Mar. Biol. 165 (6), 99. https://doi.org/10.1007/s00227-018-3354-7.
Masselink, G., Beetham, E., Kench, P., 2020. Coral reef islands can accrete vertically in response to sea level rise. Sci. Adv. https://doi.org/10.1126/sciadv.aay3656.
Masselink, G., McCall, R., Beetham, E., Kench, P., Storlazzi, C., 2021. Role of future reef growth on morphological response of coral reef Islands to sea-level rise. J. Geophys. Res. Earth 126, e2020JF005749. https://doi.org/10.1029/2020JF005749.
McKenzie, N.L., van Leeuwen, S., Pinder, A.M., 2009. Introduction to the Pilbara Biodiversity Survey, 2002–2007. Rec. West Aust. Museum. Suppl. 78, 3. https://doi.org/10.18195/issn.0313-122x.78(1).2009.003-089.
Morgan, K.M., Kench, P.S., 2014. A detrital sediment budget of a Maldivian reef platform. Geomorphology 222, 122–131. https://doi.org/10.1016/j.geomorph.2014.02.013.
Morgan, K.M., Kench, P.S., 2016. Reef to island sediment connections on a Maldivian carbonate platform: using benthic ecology and biosedimentary depositional facies to examine island-building potential. Earth Surf. Process. Landf. 41, 1815–1825. https://doi.org/10.1002/esp.3946.
Morgan, K.M., Kench, P.S., 2017. New rates of Indian Ocean carbonate production by encrusting coral reef calci fi ers : Periodic expansions following disturbance in fl uence reef-building and recovery. Mar. Geol. 390, 72–79. https://doi.org/10.1016/j.margeo.2017.06.001.

Morgan, K.M., Perry, C.T., Smithers, S.G., Johnson, J.A., Daniell, J.J., 2016. Evidence of extensive reef development and high coral cover in nearshore environments : implications for understanding coral adaptation in turbid settings. Nat. Publ. Gr. 1–10 https://doi.org/10.1038/srep29616.

Morgan, K.M., Perry, C.T., Johnson, J.A., Smithers, S.G., Morgan, K.M., Perry, C.T., 2017. Nearshore turbid-zone corals exhibit high bleaching tolerance on the great barrier reef following the 2016 Ocean Warming Event. Front. Mar. Sci. 4, 1–13. https://doi.org/10.3389/fmars.2017.00224.

Nava, H., Carballo, J.L., 2008. Chemical and mechanical bioerosion of boring sponges from Mexican Pacific coral reefs. J. Exp. Biol. 211, 2827–2831. https://doi.org/10.1242/jeb.019216.

Nilsen, J., Bonesso, J., Benson, D., Dee, S., Browne, N.K., Morgan, K., O'Leary, M., Cuttler, M., McIlwain, J., 2022. Shell crushers: Durophagous fishes turn Molluscs into Island Sediment. Reef Encount. 37 (2).

Ogston, A.S., Field, M.E., 2010. Predictions of turbidity due to enhanced sediment resuspension resulting from sea-level rise on a fringing coral reef: evidence from Molokai, Hawaii. J. Coast. Res. 26, 1027–1037. https://doi.org/10.2112/JCOASTRES-D-09-00064.1.

Palmer, S.E., Perry, C.T., Smithers, S.G., Gulliver, P., 2010. Internal structure and accretionary history of a nearshore, turbid-zone coral reef: Paluma Shoals, central Great Barrier Reef, Australia. Mar. Geol. 276, 14–29. https://doi.org/10.1016/j.margeo.2010.07.002.

Perry, C., Lange, I., Stuhr, M., 2023. Quantifying reef-derived sediment generation: introducing the SedBudget methodology to support tropical coastline and island vulnerability studies. Cambridge Prisms: Coast. Futur. 1, E26. https://doi.org/10.1017/cft.2023.14.

Perry, C.T., 1999. Reef framework preservation in four contrasting modern reef environments, Discovery Bay, Jamaica. J. Coast. Res. 15, 796–812.

Perry, C.T., Alvarez-Filip, L., 2019. Changing geo-ecological functions of coral reefs in the Anthropocene. Funct. Ecol. 33, 976–988. https://doi.org/10.1111/1365-2435.13247.

Perry, C.T., Kench, P.S., Smithers, S.G., Riegl, B., Yamano, H., O'Leary, M.J., 2011. Implications of reef ecosystem change for the stability and maintenance of coral reef islands. Glob. Chang. Biol. 17, 3679–3696. https://doi.org/10.1111/j.1365-2486.2011.02523.x.

Perry, C.T., Edinger, E.N., Kench, P.S., Murphy, G.N., Smithers, S.G., Steneck, R.S., Mumby, P.J., 2012. Estimating rates of biologically driven coral reef framework production and erosion: a new census-based carbonate budget methodology and applications to the reefs of Bonaire. Coral Reefs 31, 853–868. https://doi.org/10.1007/s00338-012-0901-4.

Perry, C.T., Murphy, G.N., Kench, P.S., Smithers, S.G., Edinger, E.N., Steneck, R.S., Mumby, P.J., 2013. Caribbean-wide decline in carbonate production threatens coral reef growth. Nat. Commun. 4, 1402–1407. https://doi.org/10.1038/ncomms2409.

Perry, C.T., Morgan, K.M., Yarlett, R.T., 2017. Reef Habitat type and spatial extent as interacting controls on platform-scale carbonate Budgets. Front. Mar. Sci. 4, 1–13. https://doi.org/10.3389/fmars.2017.00185.

Perry, C.T., Lange, I.D., Januchowski-Hartley, F.A., 2018a. ReefBudget Indo-Pacific: Online Resource and Methodology.

Perry, C.T., Alvarez-Filip, L., Graham, N.A.J., Mumby, P.J., Wilson, S.K., Kench, P.S., Manzello, D.P., Morgan, K.M., Slangen, A.B.A., Thomson, D.P., Januchowski-Hartley, F., Smithers, S.G., Steneck, R.S., Carlton, R., Edinger, E.N., Enochs, I.C., Estrada-Saldívar, N., Haywood, M.D.E., Kolodziej, G., Murphy, G.N., Pérez-Cervantes, E., Suchley, A., Valentino, L., Boenish, R., Wilson, M., MacDonald, C., 2018b. Loss of coral reef growth capacity to track future increases in sea level. Nature 558, 396–400. https://doi.org/10.1038/s41586-018-0194-z.

Putnam, H.M., Barott, K.L., Ainsworth, T.D., Gates, R.D., 2017. The vulnerability and resilience of reef-building corals. Curr. Biol. 27, R528–R540. https://doi.org/10.1016/j.cub.2017.04.047.

Rasser, M.W., Riegl, B., 2002. Holocene coral reef rubble and its binding agents. Coral Reefs 21, 57–72. https://doi.org/10.1007/s00338-001-0206-5.

Reguero, B.G., Storlazzi, C.D., Gibbs, A.E., 2021. The value of US coral reefs for flood risk reduction. Nat. Sustain. 4, 688–698. https://doi.org/10.1038/s41893-021-00706-6.

Richards, Z., Kirkendale, L., Moore, G., Hosie, A., Huisman, J., Bryce, M., Marsh, L., Bryce, C., Hara, A., Wilson, N., Morrison, S., Gomez, O., Ritchie, J., Whisson, C., Allen, M., Betterridge, L., Wood, C., Morrison, H., Salotti, M., Hansen, G., Slack-Smith, S., Fromont, J., 2016. Marine biodiversity in temperate Western Australia: Multi-taxon surveys of Minden and Roe Reefs. Diversity 8, 1–25. https://doi.org/10.3390/d8020007.

Richards, Z.T., Garcia, R.A., Wallace, C.C., Rosser, N.L., Muir, P.R., 2015. A diverse assemblage of reef corals thriving in a dynamic intertidal reef setting (Bonaparte archipelago, Kimberley, Australia). PLoS One 10, 1–17. https://doi.org/10.1371/journal.pone.0117791.

Ross, C.L., Falter, J.L., Schoepf, V., McCulloch, M.T., 2015. Perennial growth of hermatypic corals at Rottnest Island, Western Australia (32°S). PeerJ 2015, 1–26. https://doi.org/10.7717/peerj.781.

Ross, C.L., Falter, J.L., McCulloch, M.T., 2017. Active modulation of the calcifying fluid carbonate chemistry (δ11B, B/ca) and seasonally invariant coral calcification at sub-Tropical limits. Sci. Rep. 7, 1–11. https://doi.org/10.1038/s41598-017-14066-9.

Ross, C.L., DeCarlo, T.M., McCulloch, M.T., 2019. Environmental and physiochemical controls on coral calcification along a latitudinal temperature gradient in Western Australia. Glob. Chang. Biol. 25, 431–447. https://doi.org/10.1111/gcb.14488.

Roth, M.S., 2014. The engine of the reef: photobiology of the coral-algal symbiosis. Front. Microbiol. 22 (5), 422. https://doi.org/10.3389/fmicb.2014.00422. PMID: 25202301; PMCID: PMC4141621.

Ryan, E.J., Hanmer, K., Kench, P.S., 2019. Massive corals maintain a positive carbonate budget of a Maldivian upper reef platform despite major bleaching event. Sci. Rep. 9, 1–11. https://doi.org/10.1038/s41598-019-42985-2.

Sadd, J., 1984. Sediment transport and CaCO3 budget on a fringing reef, Cane Bay, St. Croix, US Virgin Islands. Bull. Mar. Sci. 35, 221–238.

Sammarco, P., Risk, M., 1990. Large-scale patterns in internal bioerosion of Porites: cross continental shelf trends on the Great Barrier Reef. Mar. Ecol. Prog. Ser. 59, 145–156. https://doi.org/10.3354/meps059145.

Schoepf, V., Baumann, J., Barshis, D., Browne, N.K., Camp, E.F., Comeau, S., Cornwall, C. E., Guzmán, H.M., Riegl, B., Rodolfo-Metalpa, R., Sommer, B., 2023. Corals at the edge of environmental limits: a new conceptual framework to re-define marginal and extreme coral communities. Sci. Total Environ. 884 https://doi.org/10.1016/j.scitotenv.2023.163688.

Silbiger, N.J., Guadayol, O., Thomas, F.O.M., Donahue, M.J., 2016. A novel µct analysis reveals different responses of bioerosion and secondary accretion to environmental variability. PLoS One 11, 11–16. https://doi.org/10.1371/journal.pone.0153058.

Spencer Davies, P., 1989. Short-term growth measurements of corals using an accurate buoyant weighing technique. Mar. Biol. 101, 389–395. https://doi.org/10.1007/BF00428135.

Stearn, W., Scoffin, T.P., 1977. Calcium carbonate budget of a fringing reef on the West Coast of Barbados. Bull. Mar. Sci. 27, 479–510.

Storlazzi, C., Elias, E., Berkowitz, P., 2015. Many atolls may be uninhabitable within decades due to climate change. Sci. Rep. 5, 14546 https://doi.org/10.1038/srep14546.

Tortolero-Langarica, J.J.A., Rodríguez-Troncoso, A.P., Cupul-Magaña, A.L., Rinkevich, B., 2020. Micro-Fragmentation as an effective and applied tool to restore remote reefs in the Eastern Tropical Pacific. Int. J. Environ. Res. Public Health 17 (18), 6574. https://doi.org/10.3390/ijerph17186574.

Toth, L.T., Courtney, T.A., Colella, M.A., Kupfner Johnson, S.A., Ruzicka, R.R., 2022. The past, present, and future of coral reef growth in the Florida Keys. Glob. Chang. Biol. 28, 5294–5309. https://doi.org/10.1111/gcb.16295.

Tribollet, A., Decherf, G., Hutchings, P.A., Peyrot-Clausade, M., 2002. Large-scale spatial variability in bioerosion of experimental coral substrates on the Great Barrier Reef (Australia): importance of microborers. Coral Reefs 424–432. https://doi.org/10.1007/s00338-002-0267-0.

Tuck, M.E., Ford, M.R., Kench, P.S., Masselink, G., 2021. Sediment supply dampens the erosive effects of sea-level rise on reef islands. Sci. Rep. 11, 1–10. https://doi.org/10.1038/s41598-021-85076-x.

Yamano, H., Miyajima, T., Koike, I., 2000. Importance of foraminifera for the formation and maintenance of a coral sand cay: Green Island, Australia. Coral Reefs Ecosyst. Transit. 19, 51–58.

Yamano, H., Kayanne, H., Chikamori, M., 2005. An overview of the nature and dynamics of reef Islands. Glob. Environ. Res. 9, 9–20.